NUCLEAR INSTRUMENTS AND METHODS 97 (1971) 299–307; © NORTH-HOLLAND PUBLISHING CO.

ELEMENTAL ANALYSIS BY ELASTIC SCATTERING*

R. K. JOLLY and H. B. WHITE, Jr.

Cyclotron Laboratory, Michigan State University, East Lansing, Michigan 48823, U.S.A.

Received 15 July 1975

It is shown that elastic scattering of an intermediate mass projectile like an α-particle is an efficient way of determining the elemental composition of any material (biological, environmental, geological, metallurgical, etc.) in one measurement. This method is particularly suitable for detecting heavy elements ($A > 16$) in the presence of a bulk of light elements and also for determining the elemental composition of biological matter. In the former case sensitivities for detecting heavy elements in atomic concentrations of 10^{-6} to 10^{-9} are easily achieved with measurement times of the order of a few tens of minutes on several currently operational Van de Graaff and cyclotron accelerator facilities. Higher sensitivities are possible at beam currents much greater than a microampere. Results of elemental analysis on specimens of whole fish, whole human blood and cow's milk are presented.

1. Introduction

It has been shown[1,2]) that the nuclear scattering technique can be profitably employed for elemental analysis of materials. The technique is particularly suitable for detecting and measuring heavy elements in the presence of a bulk of light elements because:

a) The energy of a particle elastically scattered from a light element is smaller than that of a particle scattered from a heavy element.

b) The inelastic scattering process and energy degradation of the incident beam at beam defining slits etc., both give particles only in the low energy part of the spectrum. This means that in the absence of any external background (cosmic rays, ambient radioactivity, etc.) the sensitivity for detecting the most energetic particles (scattered form the heaviest elements) is quite high.

The object of the present paper is to examine the scattering process in some detail, with a view to understanding the conditions that enable one to achieve maximum sensitivity and efficiency in its application to elemental analysis. In the following sections it is shown that the chief value of the elastic scattering technique lies in the fact that, unlike conventional techniques, one can get information about all the elements in the sample in one good energy resolution measurement. However, analysis by this technique requires access to a low energy nuclear scattering facility. Quite a few of such facilities are within easy reach of several laboratories.

In the following section, we briefly describe the nuclear scattering process. Also presented are estimates of the energy resolution required to identify the various elements in samples of varying complexity. Examples of elastically scattered α-particle spectra from thin film deposits of whole fish, human blood and milk are presented and discussed in section 4.

* Work supported by the National Science Foundation.

2. Nuclear scattering

In the nuclear scattering technique, the sample to be analysed is bombarded by projectiles of mass m and energy E_{inc}. After an elastic collision with an atomic nucleus of mass A, the incident particle emerges with an energy loss $\Delta E = E_{scatt} - E_{inc}$ which can be shown to be given by

$$\Delta E = 2E_{inc}/(1 + A/m) \qquad (1)$$

for a scattering angle of 90° (chosen for simplicity); i.e. it depends on the ratio of the masses of the incident projectile and the target nucleus and also the incident energy. Thus, for a given E_{inc} and m one can measure the mass A of the target nucleus by measuring ΔE, the energy lost in the scattering process. The mass A of the target nucleus does not tell one anything about the element the nucleus belongs to except in a few cases of mono-isotopic elements. However, each element has a characteristic isotopic abundance which serves as its signature (both in terms of the average atomic mass of the element and the relative abundance of its isotopes).

A plot of E_{scatt}/E_{inc} vs scattering angle both for protons ($m = 1$) and α-particles ($m = 4$) is shown in fig. 1 for various atomic masses. As expected, the energy loss upon scattering is appreciably greater for α-particles as compared to that for protons, particularly for lighter nuclei, indicating that the α-particle scattering is a more sensitive probe for differentiating masses of neighboring elements. An index of the sensitivity of a nuclear scattering measurement for separating nuclei of diffe-

rent masses is the mass resolution. This can be defined as the rate of change of E_{scatt} with A and for scattering at 90° can be written as

$$\Delta E_{scatt}/E_{inc} = 2m/(A+m)^2. \quad (2)$$

Here ΔE_{scatt} is the energy difference between particles scattered from two nuclei that differ by $\Delta A = 1$ mass unit. ΔE_{scatt} is, therefore, the energy resolution required to separate two nuclei that differ by 1 mass unit. Table 1 gives values of ΔE_{scatt} for both protons and α-particles of $E_{inc} = 20$ MeV, for $A = 25$, 50, 100, and 200 a.m.u. and at $\theta = 40°$, 80°, and 120°. It is apparent that the energy resolution requirements for protons are three to four times as stringent as those for α-particles of the same energy. The energy resolution capabilities of modern low-energy nuclear scattering facilities are typically $\Delta E/E \sim 1/(5\times 10^3)$ which means that the energy resolution, $\Delta E = 4$ keV for 20 MeV particles. Table 1 shows that for α-particles this is quite adequate for a mass resolution of $\Delta A = 1$ at $A = 200$ and $\theta \geq 120°$ even after allowing ~5 keV contribution to energy resolution from target thickness effects. However, a mass resolution of $\Delta A = 1$ at $A = 200$ is almost never necessary. As we shall see later, one can greatly increase the efficiency of the measurement by a suitable choice of the scattering angle where the mass resolution is just adequate for separating the various elements of interest.

In addition to the higher mass resolution achieved by using α-particles in preference to protons, there are

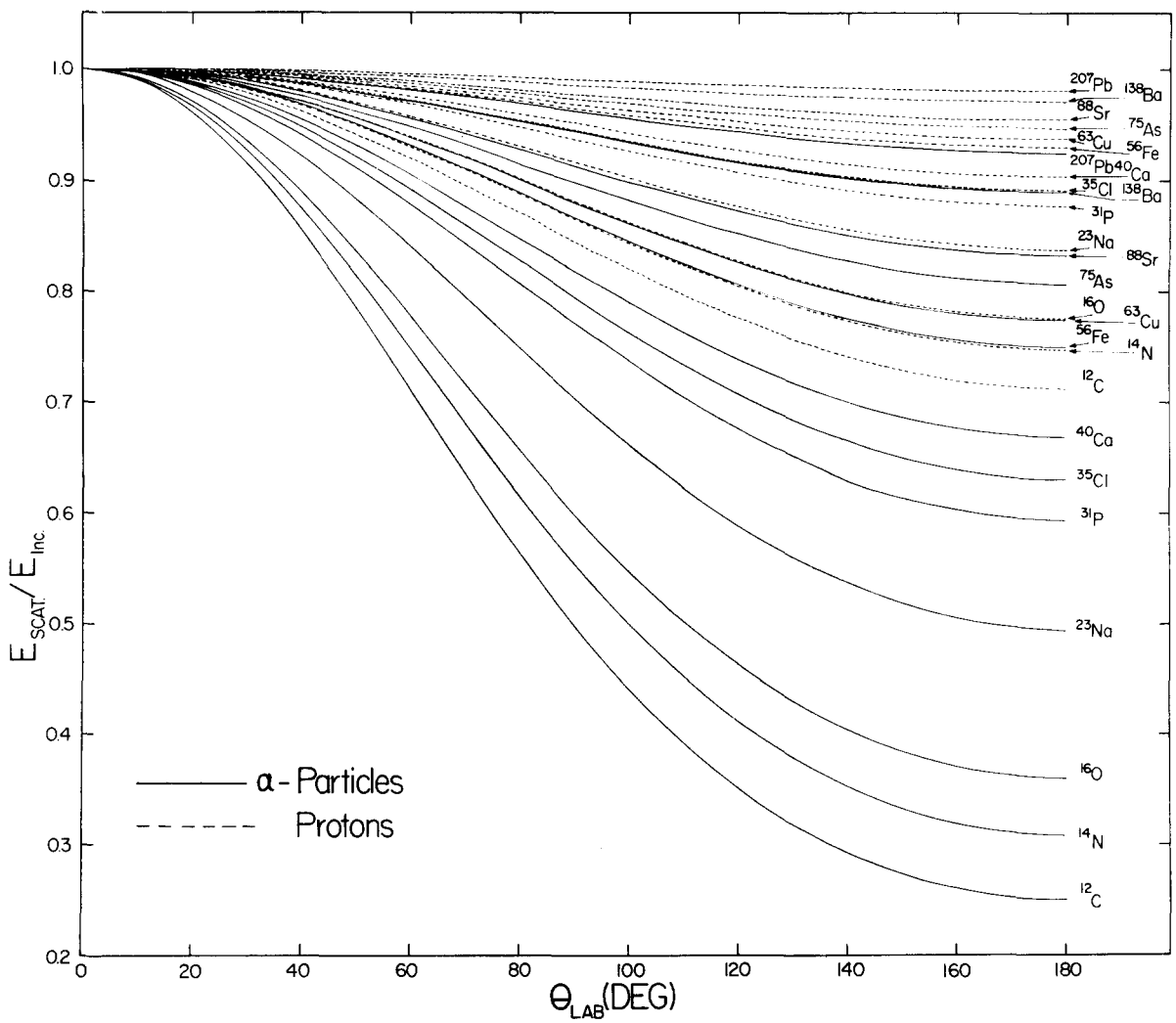

Fig. 1. Comparison of the kinematic energy loss suffered by α-particles and protons upon scattering at different angles from nuclei of different masses.

TABLE 1

Values of E_{scatt}(keV) for $E_{inc} = 20$ MeV for different A and scattering angles for both protons and α-particles and $\Delta A = 1$.

	Protons			α-Particles		
	120°	80°	40°	120°	80°	40°
$A = 25$	83	48	14	236	160	54
$A = 50$	23	12	3.7	75	46	14
$A = 100$	6	3.5	0.9	21	12	3.7
$A = 200$	1.5	0.9	0.23	5.7	3.2	0.9

TABLE 2

Differential scattering cross-sections (mb/sr) for 20 MeV α-particles and protons for ^{60}Ni, ^{120}Sn, and ^{208}Pb.

	$\theta = 40°$		$\theta = 80°$	
	α-Particles	Protons	α-Particles	Protons
^{60}Ni	366	130	5.9	20
^{120}Sn	2920	100	117	5.0
^{208}Pb	5800	500	470	40

other advantages accruing from the fact that the charge of the α-particle is twice that of the proton. These are: a) that for nearly Coulomb scattering the cross section will be greater for α-particles by a factor of 4 as compared to that for protons of the same incident energy, and b) that the Coulomb barrier is twice as high for α-particles meaning that bombarding energies near the α-particle Coulomb barrier, the inelastic α-scattering from heavy nuclei will be greatly suppressed thus minimizing the background for detecting elements somewhat lighter than the heaviest elements present in the sample. These points together with the fact that the Coulomb scattering cross-section increases as $1/E^2$, suggest that E_{inc} should be the lowest energy that will enable one to separate all the elements of interest in a sample.

However, there is a price to be paid for the choice of α-particles in that their specific energy loss, dE/dx, in all materials is 10 times that for protons of the same energy (20 MeV). [The situation is much worse in the case of heavier ions like ^{16}O. This fact together with the present unavailability of heavy ion beams of sufficient intensity and techniques for detecting heavy ions with good energy resolution has led the authors to abandon the exploration of heavy ions for use in the present measurements.] This means that the thickness of the sample and, therefore, the yield (purely from the target thickness standpoint) will be lower by a factor of ten for α-particles to maintain the same energy loss as in the case of protons so that the overall energy resolution is the same for both particles. The yield, however, also depends on the scattering cross-sections which have been compared for 20 MeV α-particles[3-10]) and protons[11]) in table 2 for nuclei of masses $A = 60$, 120, and 208. It is highly unlikely that a typical sample will contain all the elements (particularly the very heavy elements) in the periodic table in equal abundance. Table 3 shows a more probable list of elements of comparable abundance in a

TABLE 3

Energies of scattered α-particles for an incident energy = 20 MeV. Column 3 lists the energy differences of α-particles scattered from consecutive elements.

Target nucleus	E_{scatt} at 40° (MeV)	ΔE at 40° (keV)
^{207}Pb	19.8193	
		89.8
^{138}Ba	19.7295	
		23.3
^{127}I	19.7062	
		19.6
^{119}Sn	19.6866	
		109.4
^{88}Sr	19.5772	
		72.4
^{75}As	19.5048	
		93.1
^{63}Cu	19.4117	
		72.4
^{56}Fe	19.3393	
		258.3
^{40}Ca	19.0810	
		23.1
^{39}K	19.0579	
		105.0
^{35}Cl	18.9529	
		95.6
^{32}S	18.8573	
		35.8
^{31}P	18.8215	
		395.0
^{23}Na	18.4265	
		656·0
^{16}O	17.7705	
		301.2
^{14}N	17.4693	
		398.8
^{12}C	17.0705	

typical sample (only the most abundant isotopes in these elements have been tabulated). All the elements in such a sample can be easily resolved from one another at 40° with an energy resolution much poorer than that routinely achieved (10–15 keV) in several low energy nuclear physics laboratories. If several neighboring, very heavy, elements are present then the measurements have to be made at a larger angle like 80° (table 4)

TABLE 4

Energies of scattered α-particles with an incident energy of 20 MeV. Column 3 lists the energy differences of α-particles scattered from consecutive elements.

Target nucleus	E_{scatt} at 80° (MeV)	ΔE at 80° (keV)
^{207}Pb	19.3692	
		21.8
^{200}Hg	19.3474	
		9.8
^{197}Au	19.3376	
		276.9
^{138}Ba	19.0607	
		79.4
^{127}I	18.9813	
		66.7
^{119}Sn	18.9146	
		368.9
^{88}Sr	18.5457	
		241.4
^{75}As	18.3043	
		307.1
^{63}Cu	17.9972	
		236.6
^{56}Fe	17.7606	
		38.3
^{55}Mr	17.7223	
		788.9
^{40}Ca	16.9334	
		72.5
^{39}K	16.8609	
		328.1
^{35}Cl	16.5328	
		294.9
^{32}S	16.2379	
		109.8
^{31}P	16.1281	
		1178.9
^{23}Na	14.9492	
		1841.5
^{16}O	13.1077	
		800.4
^{14}N	12.3073	
		1019.4
^{12}C	11.2879	

to resolve these elements. At both of these angles the α-particle scattering cross-sections for the heavy elements (Pb–Sn) are at least an order of magnitude greater (table 2) than the proton scattering cross-sections, so that the loss in yield due to a smaller target thickness is cancelled by the increase in yield due to the larger α-scattering cross-sections. However, the advantages of greater mass resolution and the low inelastic scattering background due to the higher Coulomb barrier for α-particles still remain.

Another factor that needs consideration is the kinematic "line" broadening of monoenergetic α-particles after scattering from a light atomic nucleus. This is due to the finite angular acceptance of the detection system. Thus, when large solid angles are to be used (as is necessary for greater efficiency), some cancellation of kinematic broadening is necessary and is achieved by using a magnetic spectrograph[12]).

The largest solid angle that has been used with adequate kinematic compensation on the Enge split-pole spectrograph in the Michigan State University Cyclotron Laboratory is 4×10^{-3}sr. Table 5 shows

TABLE 5

Count-rate/h for an impurity of mass = A, abundance = 10^{-6} in an organic matter (avg. $A=10$) target (thickness = 100 μg/cm²) for 20 MeV $^4He^{++}$ beam; intensity = 1.0 μA; solid angle = 4×10^{-3} sr.

	$\theta_{LAB}=40°$	80°
$A=60$	2.5×10^2	5
$A=120$	2×10^3	10^2
$A=208$	5×10^3	5×10^2

the number of counts/h for an organic target of thickness 100 μg/cm² and an impurity of mass = A and fractional atomic abundance 10^{-6}. The scattering cross-sections used are taken from table 2. It is apparent from an examination of table 5 that, for samples typified by table 3, atomic concentrations of various elements to the levels of 10^{-6} to 10^{-8} can be measured in an hour with 1 μA of beam intensity. (Approximately 10–100 counts are needed to identify an element depending on whether it is monoisotopic or not.) However with a high intensity source that delivers 100 μA of current (such sources are becoming available) concentrations of the order of $10^{-9}-10^{-11}$ can be measured in an hour. Higher beam intensities, however,

need special handling to avoid thermal damage to the thin film targets. A high speed (up to 10000 rpm) rotating sample holder[13]) is in principle capable of solving the thermal damage problem at beam intensities $\gg 1\ \mu$A. Its usefulness at 100 μA of 10–20 MeV α-particles remains to be tested.

3. Measurements and analysis

Examples of measurements of elemental composition of whole human blood, milk, whole fish and a composite elemental target are presented and discussed in this section. The composite target was used primarily to generate a mass calibration curve for the whole fish spectrum, and was prepared by evaporation of Au, Zn and Mg on a substrate of Formvar. Thin targets of whole fish, human blood and milk were prepared also on a backing of Formvar using an ultrasonic probe and a nebulizer. Details of this technique have been discussed elsewhere[14]) and, therefore, will not be repeated here.

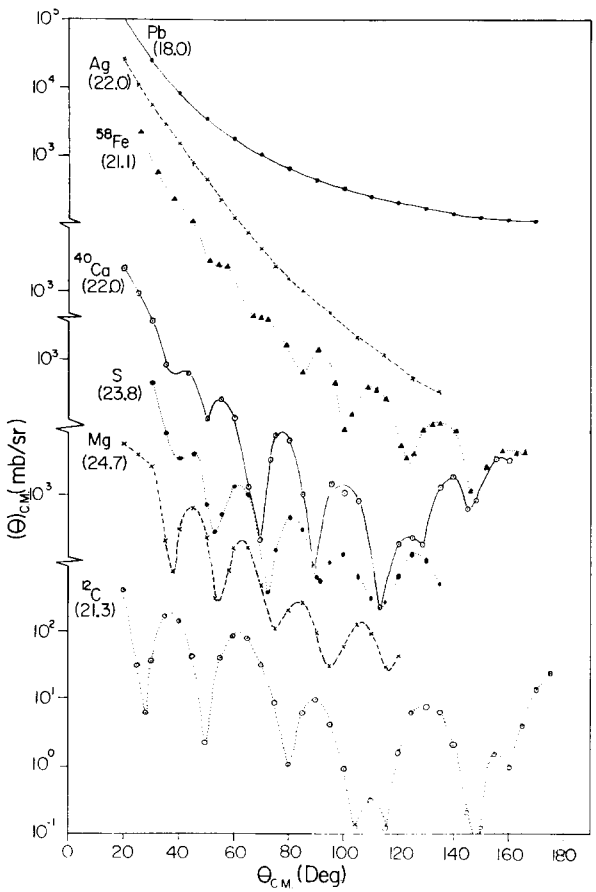

Fig. 2. A compilation of α-particle elastic scattering cross-sections for ^{12}C, Mg, S, ^{40}Ca, ^{58}Fe, Ag and Pb at the incident particle energies shown within parentheses. The data for these elements were taken from refs. 3–10.

The four targets mentioned above were bombarded with 22 MeV α-particles (the lowest energy α-particle beam currently available from the MSU Cyclotron) and the scattered particles were analysed either with a solid state surface barrier counter telescope or a magnetic spectrograph. In the case of the counter telescope, the front counter ($\sim$300 μm Si) was a totally depleted detector thick enough to stop the most energetic α-particles while other less ionizing particles went through the first detector (most of them losing a very small amount of energy in it) and were stopped in the second detector. The pulses from the second detector were used to reject all pulses in the first detector that did not originate from α-particles.

For measurements with the Enge split-pole spectrograph, the α-particle tracks were recorded in Kodak NTA nuclear emulsion plates where the reaction products were distinguished from α-particles either by the different grain density of their tracks or their reaction Q-values. Ilford K-1 plates are preferable for the present application. Unfortunately, these plates were not available at the time of the present measurements.

The atomic concentration of an element in the sample is determined from the observed elastic scattering yield, Y, by measuring the total number of incident α-particles N_0, their scattering cross-section at the incident energy $\sigma(\theta,E)$ and the solid angle, dΩ, of the detection equipment, i.e.

$$\text{Number of atoms of element of interest unitarea} = \frac{Y}{\sigma(\theta, E)\, \mathrm{d}\Omega\, N_0}. \qquad (3)$$

Thus a knowledge of the scattering cross-section at the incident α-particle energy is necessary. Unfortunately the number of α-scattering cross-section measurements at or near the 22 MeV bombarding energy is limited. Fig. 2 shows the angular distributions of elastically scattered particles from several elements spanning most of the periodic table. For heavy elements the ratio of the scattering cross-section to the Coulomb scattering cross-section does not change very rapidly from element to element so that approximate values of the scattering cross-section may be estimated for elements not shown in fig. 2 .For more accurate analysis, a library of α-scattering cross-sections is essential. Good sets of optical model parameters for α-particles of various energies incident on the most commonly observed elements in various materials may also prove to be equally useful.

It may be noted that for the heavier elements the scattering cross-section (and, therefore, the detection sensitivity for that element) increases rapidly as we go to very forward angles. But simultaneously with this increase there is a decrease in the energy separation of the α-particles scattered from the various elements in a given sample (see tables 3 and 4). Also note the large oscillations in the cross-sections for the light elements. The latter fact is very significant in biological samples where C and O are usually very abundant. As a result, in a scattering measurement on a biological sample one may see overwhelming numbers of C and O scattering events possibly masking relatively weak peaks from neighboring elements and also subjecting the solid state counter (if one does not have access to a magnetic spectrograph) to excessive radiation damage if the measurement is primarily seeking traces of heavy elements. Fig. 2 shows that by a suitable choice of a forward scattering angle (e.g. 44° at 21.3 MeV) one may simultaneously increase the yield from the heavy elements and reduce that from C. In other words the best choice of scattering angle for biological samples may be the smallest angle where the various elements of interest are still resolved and where the cross-sections for C and O go through a minimum.

However, if one has access to a magnetic spectrometer, the efficiency of these measurements can be increased by an order of magnitude or more by exploiting both the kinematic compensation and the higher energy resolution (and therefore the possibility of making the same measurements at a still smaller angle like 28° at $E_\alpha = 21.3$ MeV with a consequent large gain in the scattering cross-section) capabilities of a magnetic spectrograph. Since most samples contain a wide range of masses, for simultaneous kinematic compensation for all elements, the focal plane has a very unusual orientation, particularly for large scattering angles. The spectrograph plate holder has, therefore, to be designed keeping this limitation in mind. The plate holder in the MSU Cyclotron Laboratory was not designed for the present application and, therefore, we could not achieve complete kinematic compensation for the lighter elements in the fish and the mass calibration spectra presented in the section below.

4. Results

The first two spectra presented below (whole human blood and cow's milk) were measured with a counter telescope while the last two measurements (composite calibration target and a sonicated whole fish sample) were made with a magnetic spectrograph.

Human blood: A spectrum of the elastically scattered 22 MeV α-particles from a thin target (thickness ~40 μg/cm²) of human blood deposited on a backing of Formvar is shown in fig. 3. Some of the carbon and oxygen in the spectrum is from the backing. Quite a few elements heavier than $A = 16$ are seen. Most prominent are ^{23}Na, Cl, ^{31}P, Ca, Fe and Pb. The question mark near Pb and Ba simply means that the element identification may be somewhat uncertain due to the limited mass resolution in this part of the spectrum. The mass resolution is limited on account of the small scattering angle and the fact that there is no kinematic compensation in measurements made with a solid state detector. That is why a small solid angle (2×10^{-4} sr) was adopted for the solid state detector measurements as a compromise between efficiency and

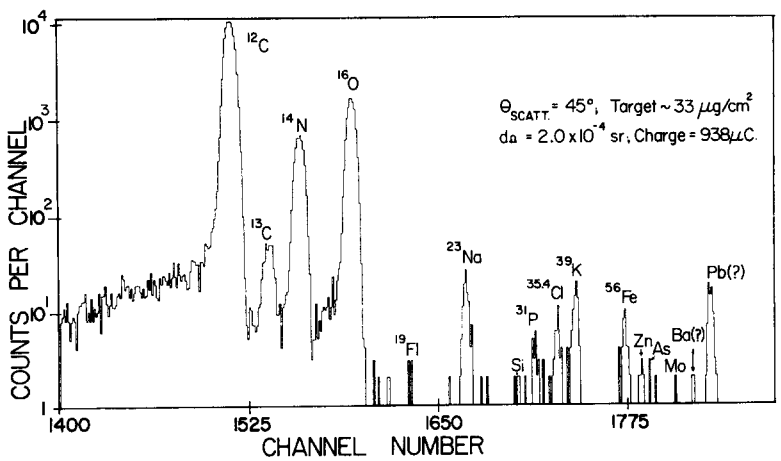

Fig. 3. Elastic scattering of 22 MeV α-particles from a ~ 33 μg/cm² deposit of whole human blood on Formvar. See text for details of extracting abundances of various elements in the blood sample (solid state counter telescope spectrum).

kinematic broadening (the broadening is particularly noticeable in the elastic peaks from ^{12}C, ^{14}N, and ^{16}O).

A comparison between the relative abundance of the various elements seen in the blood of an average human (ref. 15) and those observed in the present work in a single human blood specimen is shown in fig. 4. The two sets of data are normalized to have equal abundance of K. Agreement is reasonably good in view of the large variance of the relative elemental abundance from one sample to another[15]). The abundance measured in the present work is that of the prepared thin film sample used in the α-scattering measurement. In the process of depositing blood on Formvar, it is apparent that one loses water and probably some other substances with a very high vapor pressure at room temperature. Consequently the data obtained in the present measurement have to be corrected for this source of error. Correction has also to be applied for the fact that the deposit exists on a substrate of Formvar which might have its own heavy element impurities together with those accidentally introduced during deposition. The latter correction, however, is easily applied by making a second α-scattering measurement with pure water (same as that used in diluting the blood sample) deposited on Formvar using the same apparatus as that used in the preparation of the blood deposit. The object of the present measurements is merely to indicate the potential and the problems of the α-particle scattering technique for elemental analysis. Once the process and its peculiar features are well understood, it is hoped that standardized procedures can be easily developed to apply this technique routinely for elemental analysis of any material.

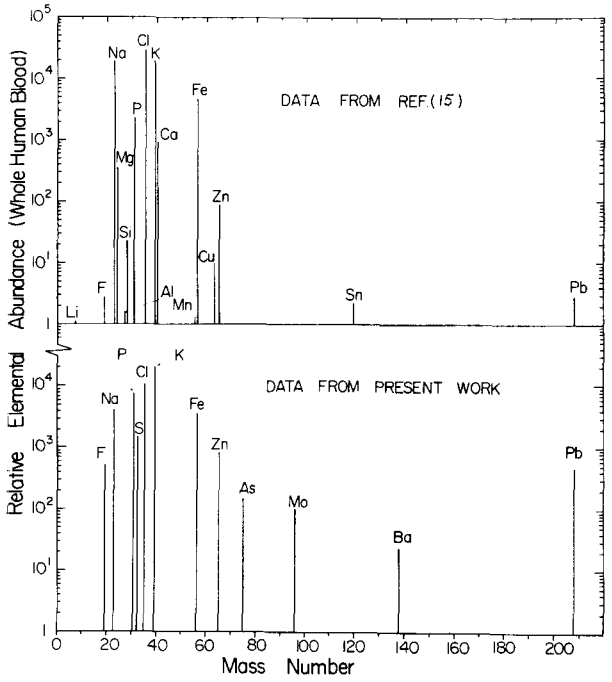

Fig. 4. A comparison of the relative abundances of various elements in whole human blood found in the present work and those obtained from ref. 15. The two sets of data are normalized to have equal abundance of K. See text for a discussion of the significance of this comparison.

Milk: An α-particle spectrum from a deposit of milk on Formvar is shown in fig. 5. This spectrum was measured with a solid state detector at a laboratory

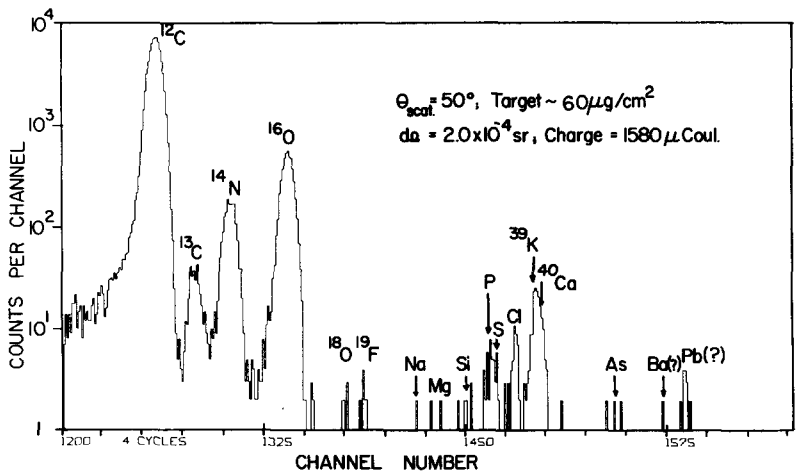

Fig. 5. Elastic scattering of 22 MeV α-particles from a ~ 60 μg/cm² target of whole cow's milk deposited on a backing of Formvar (solid state counter telescope spectrum).

angle of 45°. The most prominent peaks are those of C, N, O (an appreciable fraction of the C and O peaks are from Formvar) P, Cl and (K + Ca). But, in addition, there are also traces of F, Si, S, As and Pb(?). Both K and Ca are probably present in the spectrum in fig. 5 as the (Ca + K) peak is broader than the Cl peak. The relative abundances of most elements in fig. 5 qualitatively agree with those listed in ref. 15.

Whole fish and the composite (Au, Zn, and Mg) sample: An earlier analysis of a fish sample[16]) using the α-particle scattering technique with a surface barrier detector and also a position sensitive detector in our Enge split-pole magnetic spectrograph revealed the presence of Hg in great lakes Salmon. It was, therefore, of some interest to see what other heavy elements can be found in the same fish sample. An energy spectrum of α-particles elastically scattered from the various elements in the sample (on Formvar backing) was measured using Kodak NTA nuclear emulsion plates in the focal plane of our magnetic spectrograph. The focal plane orientation was adjusted as far as possible for simultaneous kinematic compensation for all elements from C to Pb. To obtain an "in situ" mass and/or energy calibration for the fish sample measurement, an exposure was also made with a composite thin target (~20 μg/cm² each of Au, Zn, and Mg on Formvar) in place of the fish sample. The spectrum from the composite target is shown in fig. 6 indicating the peaks from Au, Zn, and Mg in addition to those from the Formvar backing. The energy resolution for the heavy mass peaks is 11 keV (1/2 mm for 22 MeV α-particles). Of particular interest is the elastic scattering from Zn where the elastically scattered α-particles from the three even isotopes of Zn (^{64}Zn 49%, ^{66}Zn 28%, ^{68}Zn 19%) are clearly

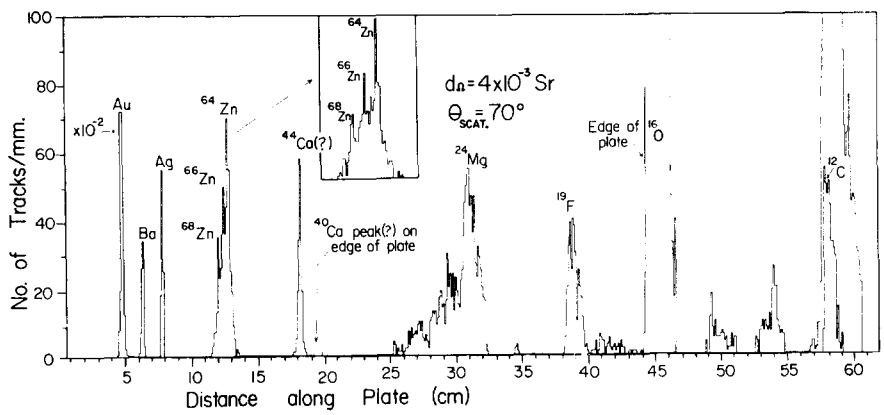

Fig. 6. Elastic scattering of 22 MeV α-particles from a thin deposit of natural Mg, Zn, and Au on a backing of Formvar. The gradual broadening of the peaks towards the light mass part of the spectrum is due to inadequate kinematic compensation for reasons of physical limitation (magnetic spectrograph spectrum).

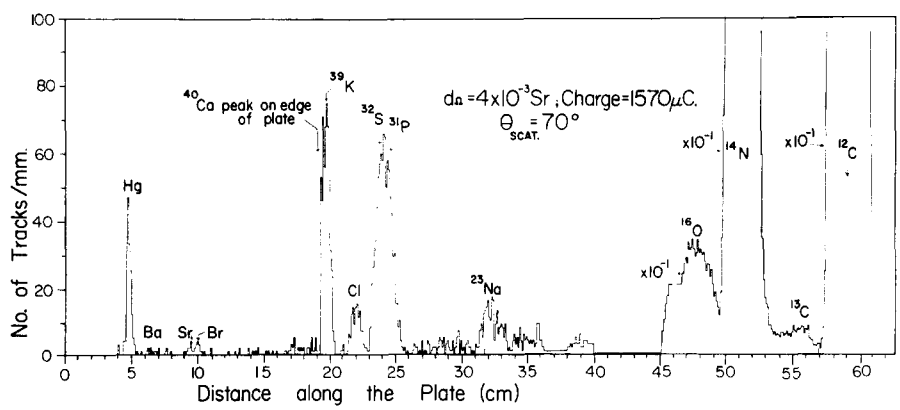

Fig. 7. Elastic scattering of 22 MeV α-particles from a thin (~ 40 μg/cm²) deposit of whole fish on Formvar. The broadening of the peaks towards the light mass part of the spectrum is due to inadequate kinematic compensation and target non-uniformity.

separated. This is one demonstration of the power of the elastic scattering technique with a high resolution device. Also note the impurity peaks like Ag and Ba not intended to be in the calibration spectrum. The fish spectrum (fig. 7) shows a fairly strong Hg peak in addition to those from K, Cl, P, Na, O, N, and C. There are also small peaks from Br, Sr, and Ba. The atomic concentration of Hg is estimated to be 0.2 ppm in the original fish specimen. The concentrations for Br and Sr are probably even greater because their scattering cross-sections (see fig. 2) at 70° are $\sim 1\%$ of the cross-section for Hg. The light mass peaks are broad because, as explained earlier, complete kinematic compensation for these peaks could not be achieved because of the physical limitation of orienting the focal plane at the unusual angle required for the above purpose. Also the Hg peak is not as narrow as some heavy element peaks in fig. 6 because Hg has several equally abundant isotopes and furthermore the fish target was not as uniform as the evaporated composite target.

The examples presented above are not meant to be accurate measurements of the elemental composition of the various substances discussed but only as illustrations of the value of the α-particle scattering technique for elemental analysis of materials.

5. Conclusion

The main points brought to a focus by the present work about the elastic scattering technique are as follows:

a) The chief value of this technique for elemental analysis lies in its ability to provide information on all the elements in a sample in one measurement at a suitably chosen angle (i.e., one commensurate with the experimental energy resolution and the elemental complexity of the sample).

b) The elastic scattering technique is particularly well suited for elemental analysis of biological samples (particularly in the areas of microbiology, pollution studies, and the role of heavy elements in the biosphere). Other techniques currently in use are severely limited in the detection of light elements whereas the α-scattering technique is particularly simple for measurement of light elements since the energy resolution requirements are the least stringent.

c) Low energy α-particle scattering offers better kinematic separation and possibly lower inelastic scattering background as compared to protons of the same energy without any loss of efficiency.

d) The sensitivity for detecting heavy elements in the presence of a bulk of light elements (e.g. Hg pollution of fish) is very high because of the practically non-existent background for the heavy elements. The limitation comes from the available beam current intensities. With the currently available intensities, concentrations of a few isolated heavy elements $\sim 10^{-7}$–10^{-8} can be measured in a few tens of minutes. In favorable cases much higher sensitivities are achievable.

e) The best α-particle energy for these studies lies in the 7–15 MeV range although the technique can also be used at much higher energies with the possibility of some interference from inelastic scattering.

The authors are particularly indebted to Professor C.R. Gruhn for help and very valuable suggestions in the initial stages of this program. The assistance of Miss M.K. Zigrang in various phases of this work is thankfully acknowledged.

References

1) B. L. Cohen and R. A. Moyer, Anal. Chem. **43** (1971) 123.
2) J. H. Patterson, A. L. Turkevich and E. Franzgrate, J. Geophys. Res. **70** (1965) 1311.
3) J. C. Corelli, E. Bleuler and D. J. Tendam, Phys. Rev. **116** (1959) 1184 and other references contained therein.
4) J. F. Morgan and R. K. Hobbif, Phys. Rev. **1C** (1970) 155.
5) H. F. Lutz and S. F. Eccles, Nucl. Phys. **81** (1966) 423.
6) M. Rahman, A. H. Khan and H. M. Sen Gupta, Nuovo Cimento **50** B, no. 1 (1967) 40.
7) G. Gregoire and P. C. Macq, Nucl. Phys. **A99** (1967) 481.
8) G. Gaul, H. Ludecke, R. Santo, H. Schmening and R. Stock, Nucl. Phys. **A137** (1969) 177.
9) H. L. Wilson and M. B. Sampson, Phys. Rev. **137** (1965) B305; also, C. B. Fulmer, J. Benveniste and A. C. Mitchell, Phys. Rev. **165** (1968) 1218.
10) M. El-Nadi and F. Riad, Nucl. Phys. **65** (1965) 99.
11) C. B. Fulmer, Phys. Rev. **125** (1962) 631.
12) H. A. Enge, Nucl. Instr. and Meth. **49** (1967) 181.
13) D. R. Maxon, R. K. Jolly and K. C. Knox, Nucl. Instr. and Meth. **62** (1968) 276.
14) R. K. Jolly and H. B. White, submitted to Nucl. Instr. and Meth.
15) *Handbook of biological data* (ed. W. S. Spevtor; Wright Air Development Center, 1956).
16) R. K. Jolly, C. R. Gruhn and C. Maggiore, Trans. Nucl. Sci. IEEE NS-**18** (1971) 19.